Spatiotemporal Optical Pulse Control Using Microwaves

H. Leblond

Laboratoire POMA, UMR 6136, Université d'Angers, 2 Bd Lavoisier, 49000 Angers, France

(Received 21 March 2005; published 15 July 2005)

The Davey-Stewartson system allows us to describe the interaction between a spatiotemporal optical pulse and adequately matched microwaves. We show that the interaction can lead to the formation of a two-dimensional soliton which is robust in the sense that it occurs in a wide range of parameters of the incident optical pulse and microwaves, and of the material used.

DOI: 10.1103/PhysRevLett.95.033902 PACS numbers: 42.65.Tg, 42.65.Jx

It is well known that optical solitons in Kerr media are unstable in more than (1 + 1) dimensions. Saturating Kerr nonlinearities or cascaded second-order ones have been considered to stabilize multidimensional pulses, an issue which is very important for applications in optical telecommunications and integrated optics. Although many advances have been made (see the review in [1]), the experimental realization of stable spatiotemporal solitons is still a challenge. We present here an alternative way of producing such structures, and show that they are robust enough, so that they are promising for experiment and applications.

In a medium presenting second-order nonlinearities, far from phase matching, the combined effect of optical rectification and electro-optic effect can efficiently affect the propagation of spatiotemporal optical pulses. It can, e.g., prevent the wave collapse [2]. It has been shown that the equations relevant to describe the propagation of a (2 + 1)-dimensional optical pulse when these effects are not neglected are of Davey-Stewartson (DS) type [3–6]. The DS system is completely integrable by means of the inverse scattering transform (IST) method for some particular values of the coefficients [7]. The elliptic-hyperbolic case, which requires anomalous dispersion, is referred to as DS I. In this case, solitons, or rather "dromions," can be formed [8,9]. The integrable case corresponds to 2 equilibriums: on one hand the cascaded second-order nonlinearities must equilibrate the third order Kerr effect; on the other hand, the dispersion has to be compared to the difference between the group velocity of the pulse and the speed of the rectified waves [10]. It has been proved numerically, in the case of electromagnetic waves in ferromagnetic media [11], but also in optics [5], that pulse stabilization was also possible in the general, nonintegrable case.

In the frame of the DS system, dromion formation requires nonzero boundary values at infinity for the auxiliary field, which describes the rectified field. This mathematical feature has been interpreted as an interaction between the pulse and solitary waves, whose length is comparable to the size of the pulse [11]. One condition is that the solitary waves travel slower than the pulse. In the optical case, numerical values can be obtained from published experimental data [12]. For potassium dihydrogen phosphate (KDP), e.g., the group velocity of the optical pulse is $v_g(\omega) \simeq 1.95 \times 10^8$ ms^{-1}, while the speed of the solitary waves is $c/n(0) \simeq 0.65 \times 10^8$ ms^{-1}; for the lithium niobate, we get: $v_g(\omega) \simeq 1.2 \times 10^8$ ms^{-1} and $c/n(0) \simeq 0.5 \times 10^8$ms^{-1}. Thus pulse control through the solitary waves should be possible [13]. However, dromion formation requires a solitary wave with a single oscillation, which is even not symmetric when the sign of the electric field is changed. This is quite difficult to realize in the microwave range. Therefore, we study in the present Letter the interaction of a (2 + 1)-dimensional optical pulse with plane waves at microwave frequency, described by the DS system. This situation is related to the formation of solitons in periodic potentials [14], with two essential differences: first the optical rectification considered in the present

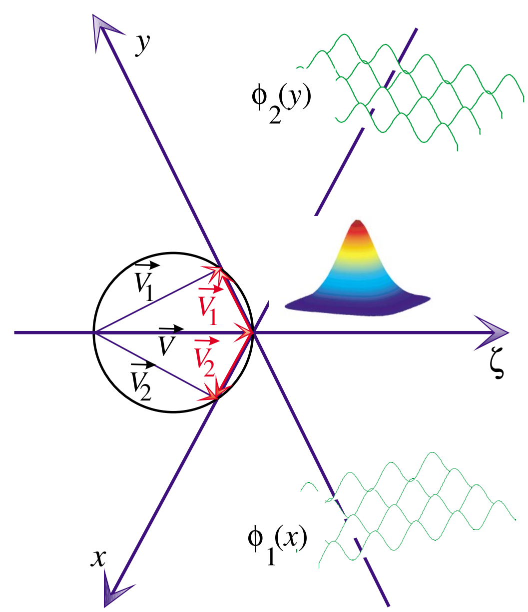

FIG. 1 (color online). The matching conditions for the interaction. $\vec{V}_1$, $\vec{V}_2$, and $\vec{V}$ are the velocities of the plane waves at microwave frequency and of the optical pulse, respectively. x and y are the characteristic coordinates of the DS model.

Letter yields a retroaction of the optical pulse to the potential, which is completely absent from the other situation. Second, we deal here with a spatiotemporal problem, while the periodic potentials considered in optics are usually purely spatial. Notice that, in such a 2-dimensional optical lattice, a stable $(3+1)$-dimensional optical soliton can be formed [15].

An efficient interaction requires a velocity matching, as shown in Fig. 1. The tips of vectors $\vec{V}_1$ and $\vec{V}_2$, velocities of the plane waves at microwave frequency, lie on the circle whose diameter goes from the origin to the tip of the vector $\vec{V}$, velocity of the optical pulse. Therefore, in the frame moving at the group velocity $\vec{V}$ of the optical pulse, the velocities $\vec{V}_1$ and $\vec{V}_2$ are parallel to the corresponding characteristic coordinates x and y, so that the plane waves are stationary in this frame [11]. This way, the duration of the interaction is very long, and it can be efficient even with a weak nonlinear effect.

The DS system [3,10] is, in normalized units,

$$i\frac{\partial u}{\partial \zeta} + \delta\frac{\partial^2 u}{\partial \xi^2} + \gamma\frac{\partial^2 u}{\partial \tau^2} = \chi u|u|^2 + bu\frac{\partial \phi}{\partial \xi}, \qquad (1)$$

$$\frac{\partial^2 \phi}{\partial \xi^2} - c^2\frac{\partial^2 \phi}{\partial \tau^2} = \sigma\frac{\partial |u|^2}{\partial \xi}, \qquad (2)$$

where ξ, τ, and ζ are normalized propagation distance, transverse spatial coordinate, and time variable, respectively. u is the envelope of the optical pulse and ϕ the rectified field. The constant δ is related to the diffraction and γ to the dispersion. c is mainly the relative speed of the microwaves with respect to light in the medium. χ is a nonlinear coefficient including the cubic Kerr nonlinearity and the effective one due to the cascaded second harmonic generation and back-conversion. b is a nonlinear coefficient accounting for electro-optic effect, while σ corresponds to optical rectification. See Refs. [4,10] for detailed expressions of these coefficients in the case of real materials. The second equation in system (2) is hyperbolic. This corresponds to the assumption that the speed of the microwaves in the medium is smaller than the speed of light, necessary to obtain an efficient interaction, as seen above. We assume further that $\gamma > 0$, which corresponds to normal dispersion. In the integrable case, these two conditions characterize the DS I system, for which dromions exist. We suppose also that $\chi < 0$, so that the self-phase-modulation is focusing both spatially and temporally. As it has been shown in [11], the interaction can yield a soliton-type propagation, at input powers below the threshold for self-focusing. We show below that this stabilization can be obtained using sinusoidal input microwaves instead of one-hump solitary waves, which renders the phenomenon achievable experimentally.

The DS system (1) and (2) is solved numerically using the scheme given in [16]. It uses the characteristic coordinates of the hyperbolic differential operator of the second equation (2): $x = c\tau - \xi$ and $y = c\tau + \xi$. The figures below are presented in this coordinate frame. We consider a given initial condition $u(\zeta = 0, x, y) = u_0(x, y)$, and boundary data

$$\phi_1(x, \zeta) = \phi_1(c\tau - \xi, \zeta) = \lim_{y \longrightarrow -\infty} \phi(x, y, \zeta), \qquad (3)$$

$$\phi_2(y, \zeta) = \phi_2(c\tau + \xi, \zeta) = \lim_{x \longrightarrow -\infty} \phi(x, y, \zeta). \qquad (4)$$

ϕ_1 and ϕ_2 can give account of the two incident plane waves, propagating in such a direction that the interaction is "resonant." We consider sinusoidal waves, as

$$\phi_1(x, \zeta) = A_1 \sin k_x(x - x_c - V_x\zeta) + B_1, \qquad (5)$$

$$\phi_2(y, \zeta) = A_2 \sin k_y(y - y_c - V_y\zeta) + B_2, \qquad (6)$$

as x or y tends to $-\infty$, that is, numerically, at the boundary of the grid. Constants B_1, B_2 are defined so that ϕ is continuous on this boundary. The initial input for the light pulse is the Gaussian

$$u_0 = A_u \exp\left(-\left(\frac{x^2}{r_x^2} + \frac{y^2}{r_y^2}\right)\right). \qquad (7)$$

For certain values of the parameters, we observe the stabilization, as shown on Fig. 2.

The question of the robustness of the obtained "driven soliton" when the input parameters are changed then arises. To discuss it, we define a pulse radius as $r = \sqrt{\langle(\vec{x} - <\vec{x}>)^2\rangle}$, where $\langle f\rangle$ is the average value of f defined by

$$\langle f\rangle = \frac{\int |u|^4 f dxdy}{\int |u|^4 dxdy}.$$

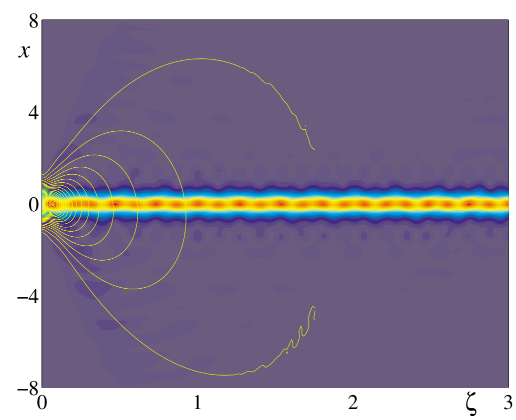

FIG. 2 (color online). Stabilization of the pulse due to the interaction: density plot in the plane $x = y$. Yellow lines indicate the pulse diffraction and dispersion in the absence of input microwaves. Parameters are: $\sigma = 1$, $\delta = 1$, $\gamma = 1$, $b = -0.6$, $c = 1$, $\chi = -1$, $A_u = 3$, $a_p = a_m = 4$, $A_1 = A_2 = 8$, $k_x = k_y = 0$, $x_c = y_c = 0$, $V_x = V_y = 0$.

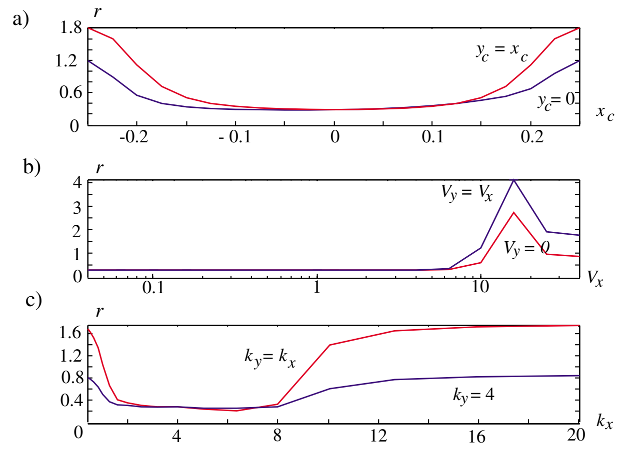

FIG. 3 (color online). Dependence of the pulse radius r after a propagation distance $\zeta = 0.4$, with regard to (a) the phases x_c, y_c, (b) the velocity mismatches V_x, V_y, (c) the wave numbers k_x, k_y of the microwaves. The parameters which are not explicitly specified on the figure are the same as in Fig. 2.

The exponent 4 is chosen to ensure that the integrals converge fast enough so that their numerically computed values do not depend on the size of the numerical box. The radius r after a given evolution time is computed and plotted against the parameters. Results are shown in Figs. 3, 5, and 6.

Figure 3(a) shows the dependence of the pulse radius with regard to the phase of the microwave. Stabilization occurs when the pulse is located at the zeros of the microwaves, while defocusing occurs when it is located at the maxima of amplitude. But the range in which stabilization occurs is very wide, more than a half period. Figure 3(b) shows the effect of a velocity mismatch. It is seen that stabilization still occurs up to a rather large value of the mismatch: $V_x, V_y \simeq 4$ in normalized units. The velocity mismatches in directions x and y operate independently one from the other, as shows the comparison between the two curves of Fig. 3(b), one corresponding to $V_y = V_x$, while for the other curve, one of the velocity mismatches is zero. The pulse is driven at the velocity of the microwave pattern, as shown on Fig. 4. The range of the wave numbers of the microwaves which yield the stability is shown in Fig. 3(c). It is reasonably large.

Figure 5(a) shows the dependence of the pulse radius with regard to the pulse width r_x, for a fixed peak amplitude, in two cases: $r_y = r_x$, then r_x is the radius of the input pulse, and r_y fixed, then we obtain in fact the dependence of the pulse radius with respect to the ellipticity of the spatiotemporal shape of the pulse. It is seen that stabilization occurs even with a rather important ellipticity. The second decrease of the pulse radius can be interpreted as the pulse collapse when its total energy exceeds some threshold. The range of pulse radius for which stabilization occurs is finite, but still reasonably large. The dependence

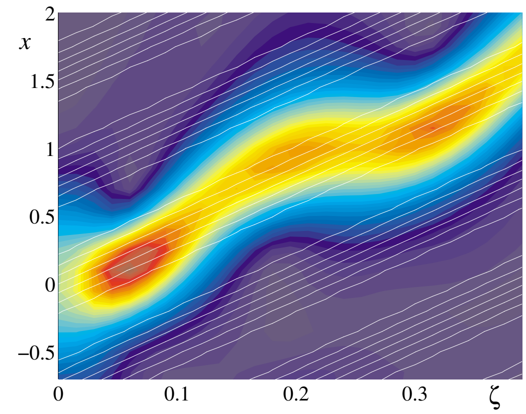

FIG. 4 (color online). Evolution of the spatial profile of the pulse during the propagation for a velocity mismatch $V_x = 4$, $V_y = 0$. The white lines show the displacement of the input microwaves. Other parameters are as in Fig. 2.

of the pulse radius with regard to the pulse amplitude A_u is shown on Fig. 5(b). When the power is increased, the pulse radius r oscillates during the propagation. This is responsible for the oscillations of the curve Fig. 5(b). The range of stabilization still appears on the plot; it is reasonably wide: $|A_u|^2$, which is proportional to the pulse energy, can go from about 14 to about 50. For larger values of A_u collapse occurs. Figure 5(c) presents the dependence of r versus the amplitude $A_1 = A_2$ of the microwaves. For small values of the amplitude A_1, diffraction and dispersion occur, as shows the plot of the final value of r at the left of Fig. 5(c). This gives a lower bound of the stabilization range about $A_1 \simeq 4$. The behavior is different when the amplitude of the microwaves is increased. The oscillations become wider and wider, but no collapse nor spreading out occurs. The range of stabilization cannot be found as easily

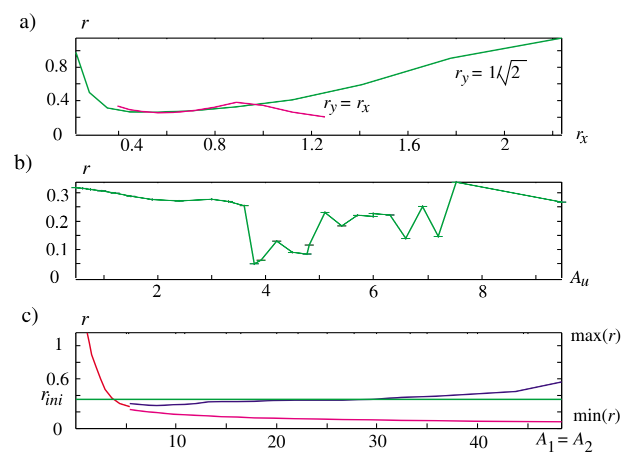

FIG. 5 (color online). Dependence of the pulse radius r after a propagation distance $\zeta = 0.4$, with regard to (a) the initial radius of the pulse r_x or r_y, (b) the pulse amplitude A_u, (c) the amplitude $A_1 = A_2$ of the microwaves. The parameters which are not explicitly specified on the figure are the same as in Fig. 2.

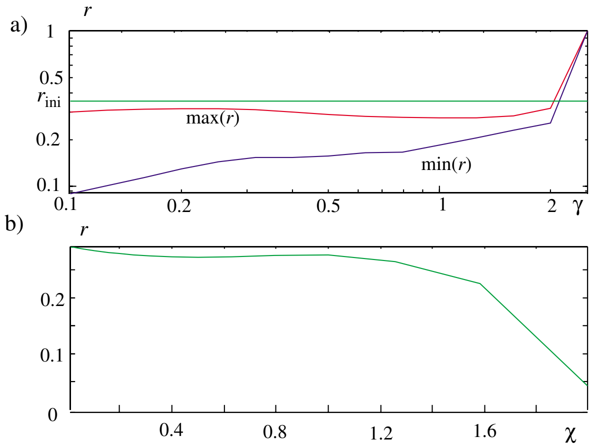

FIG. 6 (color online). Dependence of the pulse radius r after a propagation distance $\zeta = 0.4$, with regard to (a) the dispersion parameter γ and (b) the self-phase-modulation parameter χ. The parameters which are not explicitly specified on the figure are the same as in Fig. 2.

as for the parameters considered above. To overcome this difficulty, on the right part of Fig. 5(c), we represented the maximal and minimal values of the pulse radius reached during the oscillations versus the amplitude of the microwaves, and the radius r_{ini} of the input pulse. The value of $\min(r)$ shows that no collapse occurs; it has been checked that $\min(r)$ stays far enough above the discretization step. The maximum $\max(r)$, thus the amplitude of the oscillations, increases with the amplitude $A_1 = A_2$ of the microwaves. For $A_1 \lesssim 30$, the maximal value $\max(r)$ is less than r_{ini}; the oscillations tend to decrease during the propagation and the pulse can be considered as stabilized. For $A_1 \gtrsim 30$, the oscillations increase and the pulse is unstable.

The robustness of the soliton with regard to the variation of the parameters of the DS system must also be examined. The transform $\xi' = a\xi$, $\tau' = a\tau/c$, $\zeta' = \delta a^2\zeta$, $\phi' = a\phi/\sigma$, $u' = u$, with $a = \sqrt{b\sigma/(b'\delta)}$ reduces the DS system (1) and (2) to the same system with coefficients $\sigma' = \delta' = c' = 1$, b' arbitrary, $\gamma' = \gamma/(\delta c^2)$, and $\chi' = \chi b'/(b\sigma)$. Thus we can restrict our study to the coefficients χ and γ without loss of generality. The dependence of the pulse radius with regard to the dispersion coefficient γ is shown on Fig. 6(a). Spreading out occurs as γ exceeds a threshold value about 2, which gives an upper bound to the stability range. In contrast, no lower bound appears. The pulse radius r oscillates during the propagation, and as in Fig. 5(c), we have plotted the maximal and minimal values of r against γ. As γ decreases, the oscillations become larger and larger, and $\min(r)$ smaller and smaller. However, as far as the stability of the numerical scheme allows to determine it, no collapse occurs, and the oscillations decrease during the propagation. Therefore, the pulse can be considered as stabilized at least down to $\gamma = 0.1$, which is the lowest value we were able to attain numerically. Figure 6(b) shows the dependence of the pulse radius with regard to the self-phase-modulation coefficient χ. It is seen that collapse occurs when χ exceeds some threshold, while the stabilization occurs for a wide range of values of χ, and still occurs as this parameter vanishes. Thus stabilization can be achieved for a wide range of values of the parameters γ and χ, which are the only dimensionless parameters of the DS system. Therefore, the physical parameters of a wider variety of material can be expected to fall into the stabilization range.

In conclusion, we have seen that robust spatiotemporal optical pulses can thus be formed and controlled by means of adequately matched microwaves. The stabilization can be achieved for a rather large range of parameters, regarding as well the parameters of the medium, as that of the incident microwaves and optical pulse. The robustness of this phenomenon will render possible its experimental realization, opening the door to applications.

[1] B. A. Malomed, D. Mihalache, F. Wise, and L. Torner, J. Opt. B **7**, R53 (2005).

[2] L.-C. Crasovan, J. P. Torres, D. Mihalache, and L. Torner, Phys. Rev. Lett. **91**, 063904 (2003).

[3] A. Davey and K. Stewartson, Proc. R. Soc. A **338**, 101 (1974).

[4] H. Leblond, J. Phys. A **31**, 3041 (1998).

[5] M. J. Ablowitz, G. Biondini, and S. Blair, Phys. Rev. E **63**, 046605 (2001).

[6] T. Colin, Asymptotic Analysis **31**, 69 (2002).

[7] M. J. Ablowitz and H. Segur, *Solitons and the Inverse Scattering Transform* (SIAM, Philadelphia, 1981).

[8] M. Boiti, J. J.-P. Leon, L. Martina, and F. Pempinelli, Phys. Lett. A **132**, 432 (1988); M. Boiti, J. Leon, and F. Pempinelli, Inverse Probl. **6**, 715 (1990); J. Math. Phys. (N.Y.) **31**, 2612 (1990).

[9] J. Hietarinta and R. Hirota, Phys. Lett. A **145**, 237 (1990).

[10] H. Leblond, J. Phys. A **31**, 5129 (1998).

[11] H. Leblond, J. Phys. A **32**, 7907 (1999).

[12] V. G. Dmitriev, G. G. Gurzadyan, and D. N. Nikogosyan, *Handbook of Nonlinear Optical Crystals*, Springer Ser. Opt. Sci. Vol. 64, (Springer, New York, 1991).

[13] H. Leblond, in *Soliton-Driven Photonics*, edited by A. D. Boardman and A. P. Sukhorukov, NATO Science Series Vol. 31 (Kluwer, Dordrecht, 2001), p. 215.

[14] B. B. Baizakov, B. A. Malomed, and M. Salerno, Europhys. Lett. **63**, 642 (2003).

[15] D. Mihalache, D. Mazilu, F. Lederer, Y. V. Kartashov, L.-C. Crasovan, and L. Torner, Phys. Rev. E **70**, 055603(R) (2004).

[16] C. Besse and C. H. Bruneau, Math. Models Methods Appl. Sci. **8**, 1363 (1998).